CLEO CONF 97-19
EPS97 392

Measurement of New Decay Modes of the Charmed Strange Baryon Ξ_c^0

CLEO Collaboration

(July 31, 1997)

Abstract

Using the CLEO II detector operating at the e^+e^- Cornell Electron Storage Ring (CESR), we present evidence for decay modes of the Ξ_c^0 into $\Xi^-\pi^+\pi^0$, $\Xi^0\pi^+\pi^-$, and $\Xi^-\pi^+\pi^+\pi^-$. The branching ratios of these modes relative to $\Xi^-\pi^+$ have been measured to be 3.0$\pm$0.6$\pm$0.5, 2.2$\pm$0.6$\pm$0.4, and 1.8$\pm$0.6$\pm$0.5, respectively. We also set an 90% C.L. upper limit of 0.9 on the branching ratio of $\Xi^0\pi^0$ relative to $\Xi^-\pi^+$. The inclusive cross-section times the branching fraction into $\Xi^-\pi^+$ is measured to be $0.23 \pm 0.03 \pm 0.02$ pb. We find the mass splitting $\Delta M(\Xi_c^0 - \Xi_c^+)$ to be 2.5 $\pm$ 1.8 $\pm$ 1.1 MeV/c^2.

T. Bergfeld,[1] B. I. Eisenstein,[1] J. Ernst,[1] G. E. Gladding,[1] G. D. Gollin,[1] R. M. Hans,[1] E. Johnson,[1] I. Karliner,[1] M. A. Marsh,[1] M. Palmer,[1] M. Selen,[1] J. J. Thaler,[1] K. W. Edwards,[2] A. Bellerive,[3] R. Janicek,[3] D. B. MacFarlane,[3] P. M. Patel,[3] A. J. Sadoff,[4] R. Ammar,[5] P. Baringer,[5] A. Bean,[5] D. Besson,[5] D. Coppage,[5] C. Darling,[5] R. Davis,[5] N. Hancock,[5] S. Kotov,[5] I. Kravchenko,[5] N. Kwak,[5] S. Anderson,[6] Y. Kubota,[6] S. J. Lee,[6] J. J. O'Neill,[6] S. Patton,[6] R. Poling,[6] T. Riehle,[6] V. Savinov,[6] A. Smith,[6] M. S. Alam,[7] S. B. Athar,[7] Z. Ling,[7] A. H. Mahmood,[7] H. Severini,[7] S. Timm,[7] F. Wappler,[7] A. Anastassov,[8] J. E. Duboscq,[8] D. Fujino,[8,*] K. K. Gan,[8] T. Hart,[8] K. Honscheid,[8] H. Kagan,[8] R. Kass,[8] J. Lee,[8] M. B. Spencer,[8] M. Sung,[8] A. Undrus,[8,†] R. Wanke,[8] A. Wolf,[8] M. M. Zoeller,[8] B. Nemati,[9] S. J. Richichi,[9] W. R. Ross,[9] P. Skubic,[9] M. Bishai,[10] J. Fast,[10] J. W. Hinson,[10] N. Menon,[10] D. H. Miller,[10] E. I. Shibata,[10] I. P. J. Shipsey,[10] M. Yurko,[10] S. Glenn,[11] S. D. Johnson,[11] Y. Kwon,[11,‡] S. Roberts,[11] E. H. Thorndike,[11] C. P. Jessop,[12] K. Lingel,[12] H. Marsiske,[12] M. L. Perl,[12] D. Ugolini,[12] R. Wang,[12] X. Zhou,[12] T. E. Coan,[13] V. Fadeyev,[13] I. Korolkov,[13] Y. Maravin,[13] I. Narsky,[13] V. Shelkov,[13] J. Staeck,[13] R. Stroynowski,[13] I. Volobouev,[13] J. Ye,[13] M. Artuso,[14] A. Efimov,[14] M. Goldberg,[14] D. He,[14] S. Kopp,[14] G. C. Moneti,[14] R. Mountain,[14] S. Schuh,[14] T. Skwarnicki,[14] S. Stone,[14] G. Viehhauser,[14] X. Xing,[14] J. Bartelt,[15] S. E. Csorna,[15] V. Jain,[15,§] K. W. McLean,[15] S. Marka,[15] R. Godang,[16] K. Kinoshita,[16] I. C. Lai,[16] P. Pomianowski,[16] S. Schrenk,[16] G. Bonvicini,[17] D. Cinabro,[17] R. Greene,[17] L. P. Perera,[17] G. J. Zhou,[17] B. Barish,[18] M. Chadha,[18] S. Chan,[18] G. Eigen,[18] J. S. Miller,[18] C. O'Grady,[18] M. Schmidtler,[18] J. Urheim,[18] A. J. Weinstein,[18] F. Würthwein,[18] D. W. Bliss,[19] G. Masek,[19] H. P. Paar,[19] S. Prell,[19] M. Sivertz,[19] V. Sharma,[19] D. M. Asner,[20] J. Gronberg,[20] T. S. Hill,[20] D. J. Lange,[20] S. Menary,[20] R. J. Morrison,[20] H. N. Nelson,[20] T. K. Nelson,[20] C. Qiao,[20] J. D. Richman,[20] D. Roberts,[20] A. Ryd,[20] M. S. Witherell,[20] R. Balest,[21] B. H. Behrens,[21] W. T. Ford,[21] H. Park,[21] J. Roy,[21] J. G. Smith,[21] J. P. Alexander,[22] C. Bebek,[22] B. E. Berger,[22] K. Berkelman,[22] K. Bloom,[22] D. G. Cassel,[22] H. A. Cho,[22] D. S. Crowcroft,[22] M. Dickson,[22] P. S. Drell,[22] K. M. Ecklund,[22] R. Ehrlich,[22] A. D. Foland,[22] P. Gaidarev,[22] R. S. Galik,[22] L. Gibbons,[22] B. Gittelman,[22] S. W. Gray,[22] D. L. Hartill,[22] B. K. Heltsley,[22] P. I. Hopman,[22] J. Kandaswamy,[22] P. C. Kim,[22] D. L. Kreinick,[22] T. Lee,[22] Y. Liu,[22] G. S. Ludwig,[22] N. B. Mistry,[22] C. R. Ng,[22] E. Nordberg,[22] M. Ogg,[22,**] J. R. Patterson,[22] D. Peterson,[22] D. Riley,[22] A. Soffer,[22] B. Valant-Spaight,[22] C. Ward,[22] M. Athanas,[23] P. Avery,[23] C. D. Jones,[23] M. Lohner,[23] C. Prescott,[23] J. Yelton,[23] J. Zheng,[23] G. Brandenburg,[24] R. A. Briere,[24] A. Ershov,[24] Y. S. Gao,[24] D. Y.-J. Kim,[24] R. Wilson,[24] H. Yamamoto,[24]

---

[*]Permanent address: Lawrence Livermore National Laboratory, Livermore, CA 94551.

[†]Permanent address: BINP, RU-630090 Novosibirsk, Russia.

[‡]Permanent address: Yonsei University, Seoul 120-749, Korea.

[§]Permanent address: Brookhaven National Laboratory, Upton, NY 11973.

[**]Permanent address: University of Texas, Austin TX 78712

T. E. Browder,[25] Y. Li,[25] and J. L. Rodriguez[25]

[1]University of Illinois, Champaign-Urbana, Illinois 61801
[2]Carleton University, Ottawa, Ontario, Canada K1S 5B6
and the Institute of Particle Physics, Canada
[3]McGill University, Montréal, Québec, Canada H3A 2T8
and the Institute of Particle Physics, Canada
[4]Ithaca College, Ithaca, New York 14850
[5]University of Kansas, Lawrence, Kansas 66045
[6]University of Minnesota, Minneapolis, Minnesota 55455
[7]State University of New York at Albany, Albany, New York 12222
[8]Ohio State University, Columbus, Ohio 43210
[9]University of Oklahoma, Norman, Oklahoma 73019
[10]Purdue University, West Lafayette, Indiana 47907
[11]University of Rochester, Rochester, New York 14627
[12]Stanford Linear Accelerator Center, Stanford University, Stanford, California 94309
[13]Southern Methodist University, Dallas, Texas 75275
[14]Syracuse University, Syracuse, New York 13244
[15]Vanderbilt University, Nashville, Tennessee 37235
[16]Virginia Polytechnic Institute and State University, Blacksburg, Virginia 24061
[17]Wayne State University, Detroit, Michigan 48202
[18]California Institute of Technology, Pasadena, California 91125
[19]University of California, San Diego, La Jolla, California 92093
[20]University of California, Santa Barbara, California 93106
[21]University of Colorado, Boulder, Colorado 80309-0390
[22]Cornell University, Ithaca, New York 14853
[23]University of Florida, Gainesville, Florida 32611
[24]Harvard University, Cambridge, Massachusetts 02138
[25]University of Hawaii at Manoa, Honolulu, Hawaii 96822

CLEO [1] and other experimental groups [2–5] have reported the observation of the charmed-strange baryons Ξ_c^0 and Ξ_c^+. With the improved photon detection capability of the CLEO II detector, we have searched for new decay modes of Ξ_c^0, some of which involve reconstruction of a π^0 in the final state. In this report, we determine the branching ratios of Ξ_c^0 [6] decays to $\Xi^-\pi^+\pi^0$, $\Xi^0\pi^+\pi^-$ and $\Xi^-\pi^+\pi^-\pi^+$, relative to $\Xi_c^0 \to \Xi^-\pi^+$, and present an upper limit for the branching ratio of $\Xi^0\pi^0$ relative to $\Xi^-\pi^+$. This is the first measurement of the branching ratios for $\Xi^-\pi^+\pi^0$ and $\Xi^0\pi^+\pi^-$, which were among the decay modes used by CLEO to observe the Ξ_c^{*+} [7]. $\Xi^-\pi^+\pi^-\pi^+$ has been previously reported by ARGUS [5]. We use all four channels to provide the first measurement of the Ξ_c^0 fragmentation function.

Several models [8–14] predict branching fractions of $\Xi_c^0 \to \Xi^0\pi^0$ relative to $\Xi_c^0 \to \Xi^-\pi^+$. The predictions vary widely, from Körner's quark model using spin wave functions of 3% [8] to Datta's current-algebra based prediction of 359% [14]. The various models all use symmetry arguments to predict decay rates and asymmetry parameters for a wide variety of two-body charm baryon decays, so it is necessary to observe decay rates and asymmetry parameters for a large number of decays to discriminate between models.

The data sample used in this analysis corresponds to an integrated luminosity of 4.72 fb^{-1} from the $\Upsilon(4S)$ energy region and energies just below the $\Upsilon(4S)$ resonance (around 10.5 GeV), collected with the CLEO II detector [15] operating at CESR. We will describe briefly the parts of the detector relevant to this analysis. The CLEO II detector is designed to detect both charged and neutral particles with excellent resolution and efficiency. The detector consists of a charged particle tracking system surrounded by a scintillation counter based time-of-flight system and an electromagnetic calorimeter consisting of 7800 thallium-doped cesium iodide crystals. The tracking system, time-of-flight scintillators and calorimeter are installed inside a 1.5 T superconducting solenoidal magnet. The momentum resolution of the tracking system is given by $(\delta p/p)^2 = (0.15p\%)^2 + (0.5\%)^2$, where p is the track momentum in GeV/c. Charge measurements from the drift chamber wires provide specific ionization loss or dE/dx information. The photon energy resolution achieved by the electromagnetic calorimeter [16] varies from 4.2% at 100 MeV to 1.4% at 5 GeV.

Identification of hadrons is achieved by using specific ionization energy loss measurements (dE/dx) and time-of-flight (TOF) if available. By itself, the dE/dx measurement provides two standard deviation (σ) π/K separation up to 0.7 GeV/c. Time-of-flight measurements extend the 2 σ π/K separation up to 1.1 GeV/c and 2 σ p/K separation up to 1.7 GeV/c. The dE/dx and TOF measurements are combined to define a joint $\chi_i^2 = [\{(dE/dx)_{\mathrm{measured}} - (dE/dx)_{\mathrm{expected}}\}/\sigma_{dE/dx}]_i^2 + [\{(T)_{\mathrm{measured}} - (T)_{\mathrm{expected}}\}/\sigma_{\mathrm{TOF}}]_i^2$, where i corresponds to the pion, kaon, and proton hypotheses. A χ^2-probability is then calculated for each hypothesis. A charged track is defined to be consistent with a pion (proton) hypothesis, if its probability to be a pion (proton) is greater than 0.001.

At CESR energies, charmed baryons can be produced from B meson decays or directly from e^+e^- annihilations into $c\bar{c}$ jets. In this analysis, we have used the fragmentation variable x_p, defined as $x_p = p/p_{max}$, where p is the momentum of the Ξ_c^0, $p_{max}^2 = E_{beam}^2 - M_{\Xi_c^0}^2$, E_{beam} is the beam energy, and $M_{\Xi_c^0}$ is the mass of the Ξ_c^0. We limit our search to x_p greater than 0.5 to avoid the combinatorial background which dominates at low x_p. This requirement also eliminates charmed baryons from B meson decay.

The vertex of the Ξ_c^0 decay in CLEO II is indistinguishable from its production point at the event vertex. We reconstruct Ξ_c^0 by combining hyperons Λ, Ξ^0, and Ξ^-, that have well-separated vertices, with tracks from the primary event vertex. Good secondary vertices are characterized by the distance of the hyperon decay vertex from the event vertex in the $r-\phi$ plane, (required to be more than 2 mm for Λ and Ξ^-, 1 cm for Ξ^0); the difference in the z positions of the two tracks forming the vertex (required to be less than 2 cm for Λ and Ξ^-, 2.5 cm for Ξ^0), and the miss distance in the $r-\phi$ plane of the π^- extrapolated back to the vertex (more than 1 mm for Λ and 0.5 mm for Ξ^-.)

The Λ candidates are formed from pairs of oppositely charged tracks, assuming the higher momentum track to be a proton and requiring it to be consistent with the proton particle identification hypothesis. We require the invariant mass of Λ candidates to be within 5 MeV/c^2 ($\sim 2.5\sigma$) of the known Λ mass. We select Λ candidates that are decay products from Ξ^- and Ξ^0 by extrapolating the momentum vector of the Λ back to the event vertex in the $r-\phi$ plane and requiring the extrapolation to miss the vertex more than 0.3 mm and less than 10 cm. The Ξ^- candidates are formed by combining each Λ candidate with one of the remaining negatively charged tracks in the event, which is assumed to be a pion. A vertex is formed from the intersection of the Λ and the negatively charged track. Combinations of $\Lambda\pi^-$ with an invariant mass within 6 MeV/c^2 ($\sim 3\sigma$) of the measured Ξ^- mass are accepted as Ξ^- candidates.

The Ξ^0 candidates are found by forming all $\Lambda\pi^0$ combinations in the event. Candidates for good π^0's are formed from pairs of photon candidates, of which at least one is detected in the barrel CsI crystals, ($|\cos\theta| < 0.707$), where θ is the angle between the photon and the beam line. The π^0 candidates are kinematically fit to the π^0 mass and we require the χ^2 of the fit to be less than 10. We require all photon candidates to deposit at least 50 MeV in the CsI crystals and exclude showers that match charged tracks projected into the calorimeter. The Ξ^0 finding is done using a $\Xi^0\to\Lambda\pi^0$ reconstruction algorithm used in previous CLEO analyses [17]. We require the momentum of the π^0 to be greater than 70 MeV/c. Ξ^0 candidates are selected if the $\Lambda\pi^0$ invariant mass of the selected secondary vertex falls within 8.0 MeV/c^2 (3.0 σ) of the known Ξ^0 mass. Figures 1 (a), (b) and (c) show the invariant mass distributions corresponding to $p\pi^-$, $\Lambda\pi^-$, and $\Lambda\pi^0$, respectively, after the above requirements are applied. We obtain approximately 120,000 Λ, 11000 Ξ^-, and 7000 Ξ^0 candidates.

Using the Ξ^- and Ξ^0 candidates selected above, we calculate the invariant mass for the combinations $\Xi^0\pi^0$, $\Xi^-\pi^+\pi^0$, $\Xi^0\pi^+\pi^-$, $\Xi^-\pi^+\pi^-\pi^+$ and $\Xi^-\pi^+$. In each case, only combinations with $x_p > 0.5$ are included. For each primary charged pion used in the above combinations, we have required the miss distance from the primary event vertex in the $r-\phi$ plane to be less than 2 mm and z-coordinate at the closest point to the primary vertex to be less than 5 cm. The momenta of the charged and neutral pions are required to be greater than 100 MeV/c. Further, we require the particle identification information of the tracks to be consistent with the pion hypothesis as defined earlier.

We isolate the signals by requiring the angle the daughter products make with the parent Ξ_c^0 in the lab frame to be in the forward hemisphere, since the combinatorial background from the rest of the tracks tends to peak in the backward hemisphere.

In Figures 2(a)-2(d) we present invariant mass distributions corresponding to $\Xi^-\pi^+$, $\Xi^-\pi^+\pi^0$, $\Xi^0\pi^+\pi^-$, and $\Xi^-\pi^+\pi^-\pi^+$ combinations, respectively. The signal size is found by fitting each invariant mass distribution to the sum of a Gaussian function with width fixed at the Monte Carlo predicted value and a smooth low order polynomial background. From the fitting procedure, we obtain signal sizes of 83 ± 11, 84 ± 12, 50 ± 11, and 33 ± 9 events respectively.

We calculate the branching ratios of the four new modes relative to that into $\Xi^-\pi^+$, which has been reported previously by CLEO [1] and ARGUS [5]. The reconstruction efficiency in each mode is found using a GEANT-based Monte Carlo simulation [18] of the CLEO II detector. Since the mass resolution and the reconstruction efficiencies are momentum dependent, we divide the data and Monte Carlo into intervals of x_p. The reconstruction efficiency ϵ_i and the width of the peak are found for each x_p interval in the Monte Carlo. We then fit the data in the corresponding interval with a polynomial background and a Gaussian function with the width fixed to the Monte Carlo prediction to obtain the raw yield ΔY_i. The mass is fixed to be that found in the global fit to the full data. Dividing the raw yield by its corresponding efficiency, we obtain the corrected yield ΔN_i. The results for the decay modes $\Xi^-\pi^+$, $\Xi^-\pi^+\pi^0$, $\Xi^0\pi^+\pi^-$ and $\Xi^-\pi^+\pi^-\pi^+$ are presented in Tables I, II, III and IV, respectively. The summed corrected yields for $x_p > 0.5$ are also presented in the above tables. Dividing the yields of the last three decay modes above by that for $\Xi^-\pi^+$, we obtain their branching fractions relative to that into $\Xi^-\pi^+$, shown in Table V.

Figure 3 shows the invariant mass distribution for $\Xi^0\pi^0$ combinations. The signal is predicted by Monte Carlo to have a width $\sigma = 20$ MeV. Due to uncertainty in the background shape, we set a limit by assuming that all 12 events in the $\pm 3\sigma$ mass band are signal. Using Poisson probabilities and assuming no expected background, a signal of 17 events will fluctuate down to 12 events 10% of the time. Given our efficiency for signal of 1.7%, this corresponds to a 90% limit on the corrected yield of 1000 events and an upper limit on $B(\Xi_c^0 \to \Xi^0\pi^0)/B(\Xi_c^0 \to \Xi^-\pi^+) < 0.9$.

We calculate the production cross-section for Ξ_c^0 using the high statistics mode $\Xi^-\pi^+$. Since we do not know the absolute branching fraction of any Ξ_c^0 decay mode, we measure the product of cross section and branching ratio $\sigma \cdot B(\Xi_c^0 \to \Xi^-\pi^+)$ as shown below:

$$\sigma \cdot B(\Xi_c^0 \to \Xi^-\pi^+) = \frac{\sum \Delta N_i}{\mathcal{L}}, \tag{1}$$

where the summation corresponds to $x_p > 0.5$ and $\mathcal{L}$ is the integrated luminosity. Using Table I, we find $\sigma \cdot B(\Xi_c^0 \to \Xi^-\pi^+)$ for $x_p > 0.5$ to be $0.23 \pm 0.03 \pm 0.02$ pb, where the first error is statistical and the second is systematic, obtained by studying the variation of the corrected yield with changes in the analysis and from uncertainties in Monte Carlo efficiencies for tracking and secondary vertex finding.

For each decay mode, we form the normalized momentum distribution $\frac{1}{N}\frac{\Delta N_i}{\Delta x_{p_i}}$ where N is the total corrected yield for $x_p > 0.5$. In this way, the momentum distributions from the four decay channels will have the same normalization and we can take a weighted average in each momentum interval to make a joint momentum distribution. The data for the distribution is shown in Table VI. Figure 4 shows the joint normalized momentum distribution. We fit this distribution to the Peterson fragmentation function [19]

$$D_Q^h(x_p) = N\{x_p[1 - \frac{1}{x_p} - \frac{\epsilon_q}{(1-x_p)^2}]^2\}^{-1} \tag{2}$$

where ϵ_q is the fragmentation parameter and N is a normalization constant. The fit yields a value of $\epsilon_q = 0.17^{+0.04}_{-0.05} \pm 0.05$, which is similar to $0.23^{+0.06}_{-0.05} \pm 0.03$ for the Ξ_c^+ as measured by

CLEO [21]. The systematic error of 0.05 is obtained by loosening the selection requirements and observing the variation of ϵ_q. By integrating the Peterson function from 0 to 1 we find that $(68 \pm 4)\%$ of the Ξ_c^0 production occurs at x_p of 0.5 and greater.

Table VII summarizes our calculation of systematic errors. First, each of the decay modes is assigned systematics due to uncertainties in the reconstruction efficiencies for Λ, Ξ^- and Ξ^0 (4%, 3%, and 7% respectively), charged particle tracking (2% per track) and for π^0 finding (5%). In each case, a systematic error is assigned only if it involves finding a particle that is not in the $\Xi^-\pi^+$ decay mode. Second, we find the signal with an alternate and looser set of requirements, and take the variation in the corrected yield as a systematic error. Third, we divide the sample in three independent subsamples corresponding to three periods of data taking and calculate the cross-section times branching ratio in each subsample. We calculate a χ^2 that these three measurements are consistent with a single value. We do not find any variation in the measurements that is inconsistent with statistics; the limits we show represent the sensitivity of this technique and are not counted in the systematic error budget.

We investigate potential changes in the efficiency caused by resonant substructure in these decay modes by generating Monte Carlo that is 100% resonant and comparing the efficiency to that found from the nonresonant Monte Carlo which is used in calculating the branching ratios. The resonant Monte Carlo includes $\Xi^*(1530)$ and ρ resonances. In $\Xi^0\pi^+\pi^-$ and $\Xi^-\pi^+\pi^0$ we find that there is no effect on the efficiency due to the potential presence of resonances. In $\Xi^-\pi^+\pi^-\pi^+$ the efficiency due to $\Xi^*(1530)$ is considerably larger. We assign a systematic error of 23% to this channel, equivalent to the magnitude of the efficiency correction.

We measure the mass splitting between Ξ_c^0 and Ξ_c^+ by using only the kinematically similar channels $\Xi_c^0 \to \Xi^-\pi^+$ and $\Xi_c^+ \to \Xi^-\pi^+\pi^+$ so that many of the errors on our absolute mass scale cancel out [22]. Our preliminary result for the M(Ξ_c^0-Ξ_c^+) mass splitting is 2.5$\pm$1.8 MeV/c^2 [23]. We can also calculate the mass splitting by beginning with the world average masses of the D^+ and D^0 mesons for Ξ_c^+ and Ξ_c^0 respectively, and adding the measured mass differences of $\Delta M(\Lambda_c^+ - D)$ and $\Delta M(\Xi_c - \Lambda_c^+)$, in kinematically similar channels. In this way we obtain a mass splitting that is 1.1 MeV higher and we take this as our systematic error.

CLEO used measurements of the Ξ_c^0 lifetime and semileptonic decay to determine that $B(\Xi_c^0 \to \Xi^-\pi^+) = f_{SL} f_{\Xi_c^0} \times (0.0052 \pm 0.0016^{+0.0015}_{-0.0010})$ [24,25], where $f_{\Xi_c^0} \equiv B(\Xi_c^0 \to \Xi^- l^+ \nu_l)/B(\Xi_c^0 \to l^+ X) \leq 1$, (current predictions range from 0.4 to 0.9 [26,27]), and $f_{SL} \equiv (\Gamma_{SL}^{\Xi_c}/\Gamma_{SL}^{\Lambda_c})(\Gamma_{SL}^{\Lambda_c}/\Gamma_{SL}^{D})$, with Γ_{SL} being the total semileptonic width. The f_{SL} factor is introduced to adjust for the predicted differences between the semileptonic widths of the Ξ_c^0 and Λ_c^+ (2-3 times larger [28]), and between the Λ_c^+ and the D (1.5 times larger [29]). The Ξ_c^0 decay modes reported in this paper together account for 8.0 $\pm$ 1.3 times the branching ratio of $\Xi_c^0 \to \Xi^-\pi^+$, or $f_{SL} f_{\Xi_c^0} \times (4.1 \pm 1.4)\%$ of the absolute branching fraction.

In Table VIII we present a summary of theoretical predictions for the two-body decays of Ξ_c^0 observable by this study. We also present the current experimental results on these decays, converted into absolute branching fractions multiplied by the unknown factors $f_{SL} f_{\Xi_c^0}$ by using the CLEO estimates of the absolute branching fraction $\Xi_c^0 \to \Xi^-\pi^+$ described above. Our upper limit on the $\Xi^0\pi^0$ relative branching ratio indicates that the current algebra predictions of Refs [13,14] which favor a high $B(\Xi^0\pi^0/\Xi^-\pi^+)$ are disfavored. However, another current algebra prediction [11] is still consistent with the known data.

In conclusion, we have observed three Ξ_c^0 decays into $\Xi^-\pi^+\pi^0$, $\Xi^0\pi^+\pi^-$ and $\Xi^-\pi^+\pi^-\pi^+$, and have measured their branching fractions relative to that into $\Xi^-\pi^+$ to be $3.0 \pm 0.6 \pm 0.5$, $2.2 \pm 0.6 \pm 0.4$ and $1.8 \pm 0.6 \pm 0.5$, respectively. The value of $1.8 \pm 0.6 \pm 0.5$ obtained for $B(\Xi^-\pi^+\pi^-\pi^+)/B(\Xi^-\pi^+)$ is to be compared with the ARGUS value of 3.3 ± 1.4 [5,31]. We also have set an upper limit on $B(\Xi^0\pi^0\ /\Xi^-\pi^+) < 0.9$ at 90% C.L. The production cross-section $\sigma \cdot B(\Xi_c^0 \to \Xi^-\pi^+)$ is measured to be $0.23 \pm 0.03 \pm 0.02$ pb for $x_p > 0.5$, as compared to the previous CLEO measurement $\sigma \cdot B(\Xi_c^0 \to \Xi^-\pi^+) = 0.39 \pm 0.10$ pb for $x_p > 0.5$ [1].

We gratefully acknowledge the effort of the CESR staff in providing us with excellent luminosity and running conditions. This work was supported by the National Science Foundation, the U.S. Department of Energy, the Heisenberg Foundation, the Alexander von Humboldt Stiftung, Research Corporation, the Natural Sciences and Engineering Research Council of Canada, and the A.P. Sloan Foundation.

TABLE I. Inclusive $\Xi^-\pi^+$ production

Δx_p	MC Width [MeV/c^2]	Raw yield $\Delta Y_i(x_p)$	Efficiency ϵ [%]	Corrected Yield $\Delta N_i(x_p)$
$0.5-0.6$	9.8 ± 0.3	7.9 ± 4.4	6.4 ± 0.2	124.1 ± 68.4
$0.6-0.7$	9.9 ± 0.2	29.4 ± 6.3	7.5 ± 0.2	391.2 ± 84.7
$0.7-0.8$	10.5 ± 0.3	31.4 ± 5.8	7.7 ± 0.2	407.8 ± 77.0
$0.8-0.9$	11.3 ± 0.4	13.0 ± 4.0	8.3 ± 0.4	156.2 ± 49.2
$0.9-1.0$	10.3 ± 1.2	1.3 ± 1.4	6.9 ± 1.0	18.8 ± 21.1
$0.5-1.0$		83.0 ± 10.6		1098.0 ± 143.7

TABLE II. Inclusive $\Xi^-\pi^+\pi^0$ production

Δx_p	MC Width [MeV/c^2]	Raw yield $\Delta Y_i(x_p)$	Efficiency ϵ [%]	Corrected Yield $\Delta N_i(x_p)$
$0.5-0.6$	12.0 ± 1.0	19.8 ± 7.0	2.2 ± 0.2	904.1 ± 327.8
$0.6-0.7$	12.5 ± 0.6	32.9 ± 7.7	2.6 ± 0.1	1278.1 ± 306.9
$0.7-0.8$	13.1 ± 0.8	21.2 ± 6.0	2.7 ± 0.2	777.1 ± 225.7
$0.8-0.9$	13.6 ± 0.8	9.1 ± 3.4	3.4 ± 0.2	268.1 ± 101.3
$0.9-1.0$	10.9 ± 3.2	0.6 ± 1.0	2.5 ± 0.7	24.1 ± 40.9
$0.5-1.0$		83.6 ± 12.5		3251.6 ± 514.4

TABLE III. Inclusive $\Xi^0\pi^+\pi^-$ production

Δx_p	MC Width [MeV/c^2]	Raw yield $\Delta Y_i(x_p)$	Efficiency ϵ [%]	Corrected Yield $\Delta N_i(x_p)$
$0.5-0.6$	7.7 ± 0.5	7.9 ± 6.5	2.0 ± 0.1	391.9 ± 323.4
$0.6-0.7$	7.5 ± 0.5	26.9 ± 7.0	2.0 ± 0.1	1353.3 ± 359.1
$0.7-0.8$	8.9 ± 0.5	3.5 ± 3.8	2.4 ± 0.1	147.2 ± 162.1
$0.8-0.9$	8.4 ± 0.6	9.4 ± 3.8	2.2 ± 0.2	418.4 ± 174.1
$0.9-1.0$	6.9 ± 1.1	2.1 ± 1.8	2.8 ± 0.6	73.9 ± 64.8
$0.5-1.0$		49.7 ± 11.1		2384.8 ± 542.5

TABLE IV. Inclusive $\Xi^-\pi^+\pi^-\pi^+$ production

Δx_p	MC Width [MeV/c^2]	Raw yield $\Delta Y_i(x_p)$	Efficiency ϵ [%]	Corrected Yield $\Delta N_i(x_p)$
$0.5-0.6$	6.1 ± 0.6	9.6 ± 5.3	1.3 ± 0.1	769.0 ± 424.8
$0.6-0.7$	7.6 ± 0.6	8.9 ± 5.0	1.7 ± 0.1	511.7 ± 291.2
$0.7-0.8$	6.3 ± 0.5	7.8 ± 3.8	1.9 ± 0.1	406.9 ± 198.6
$0.8-0.9$	7.5 ± 0.6	5.1 ± 2.8	2.4 ± 0.2	213.8 ± 117.2
$0.9-1.0$	7.5 ± 1.2	1.7 ± 1.4	3.3 ± 0.7	51.5 ± 44.5
$0.5-1.0$		33.2 ± 8.8		1952.9 ± 566.1

TABLE V. Corrected Yields and Relative Branching Ratios

Decay Mode	Raw Yield	Corrected Yield	Ratio relative to $\Xi_c^0 \to \Xi^-\pi^+$
$\Xi^-\pi^+$	83 ± 11	1098 ± 144	1
$\Xi^-\pi^+\pi^0$	84 ± 12	3251 ± 514	$3.0 \pm 0.6 \pm 0.5$
$\Xi^0\pi^+\pi^-$	50 ± 11	2385 ± 542	$2.2 \pm 0.6 \pm 0.4$
$\Xi^-\pi^+\pi^-\pi^+$	33 ± 9	1953 ± 566	$1.8 \pm 0.6 \pm 0.5$
$\Xi^0\pi^0$	< 17	<1000 (90% CL)	<0.9 (90% CL)
	Sum (not including $\Xi^0\pi^0$)		8.0±1.3

TABLE VI. Combined Normalized Momentum Distribution

Δx_p	dN/N				Weighted
	$\Xi^-\pi^+$	$\Xi^-\pi^+\pi^0$	$\Xi^0\pi^+\pi^-$	$\Xi^-\pi^+\pi^-\pi^+$	Average
$0.5-0.6$	0.113 ± 0.064	0.278 ± 0.110	0.200 ± 0.137	0.394 ± 0.246	0.171 ± 0.050
$0.6-0.7$	0.356 ± 0.090	0.393 ± 0.113	0.483 ± 0.174	0.262 ± 0.167	0.370 ± 0.061
$0.7-0.8$	0.371 ± 0.085	0.239 ± 0.079	0.098 ± 0.074	0.208 ± 0.118	0.221 ± 0.043
$0.8-0.9$	0.142 ± 0.049	0.082 ± 0.034	0.189 ± 0.083	0.109 ± 0.068	0.111 ± 0.025
$0.9-1.0$	0.017 ± 0.019	0.007 ± 0.013	0.030 ± 0.025	0.026 ± 0.024	0.015 ± 0.009

TABLE VII. Systematic Error Summary

Mode	Corrected Yield	Statistical Error (%)	Monte Carlo Efficiency (%)	Cut Variations (%)	Data Set Variations (Not Used)(%)	Resonance Variations (%)	Total Systematics (%)
$\Xi^-\pi^+$	1098 ± 144	13%	N/A	10%	$< 4\%$	N/A	10.0%
$\Xi^-\pi^+\pi^0$	3251 ± 514	16%	5%	12%	$< 14\%$	N/A	15.6%
$\Xi^0\pi^+\pi^-$	2385 ± 542	23%	7%	13%	$< 20\%$	N/A	14.7%
$\Xi^-\pi^+\pi^-\pi^+$	1953 ± 566	29%	4%	4%	$< 11\%$	23%	23.6%

TABLE VIII. Theoretical Predictions of Ξ_c Branching Ratios (in percent)

Decay mode	[8]	[9]	[10]	[13]	[13]	[11]	[12]	[14]	Experiment$\times f_{SL} f_{\Xi_c^0}$
$\Xi_c^0 \to \Omega^- K^+$	0.29	0.13							0.26± 0.14 [30]
$\Xi_c^0 \to \Xi^- \pi^+$	0.91	1.52	2.30	1.10	0.73	0.61	0.88	0.17	0.52±0.16 [24]‡
$\Xi_c^0 \to \Xi^0 \pi^0$	0.03	0.49	0.31	0.25	1.10	0.69	0.29	0.61	<0.47 ‡
$\Xi_c^0 \to \Xi^0 \rho^0$	1.50					1.22	0.31	0.11	
$\Xi_c^0 \to \Xi^- \rho^+$	10.75					1.50	0.64	1.27	
$\Xi_c^0 \to \Xi^{*0} \pi^0$	0.25	0.11							
$\Xi_c^0 \to \Xi^{*-} \pi^+$	0.40	0.22							

‡This result

REFERENCES

[1] P. Avery et al, Phys. Rev. Lett. 62, 863 (1989); M. Alam et al, Phys. Lett. B226, 401 (1989).
[2] S. Biagi et al, Phys. Lett. B 150, 230 (1985); S. Biagi et al, Z. Phys. C28, 175 (1985).
[3] P. Coteus et al, Phys. Rev. Lett. 59, 1530 (1987).
[4] S. Barlag et al, Phys. Lett. B 236, 495 (1990).
[5] H. Albrecht et al, Phys. Lett. B 247, 121 (1990).
[6] Charge conjugate modes are implied throughout the entire discussion.
[7] L. Gibbons et al, Phys. Rev. Lett. 77, 810 (1996).
[8] J.G. Körner and M. Kraemer, Z. Phys. C 55, 659 (1992).
[9] Q.P. Xu and A.N. Kamal, Phys. Rev. D 46, 270 (1992); Q.P. Xu and A.N. Kamal, Phys. Rev. D 46, 3836 (1992).
[10] T. Uppal, R.C. Verma and M.P. Khanna, Phys. Rev. D 49, 3417 (1994).
[11] P. Żenczykowski, Phys. Rev. D 50, 5787 (1994).
[12] P. Żenczykowski, Phys. Rev. D 50, 402 (1994).
[13] H. Cheng and B. Tseng, Phys. Rev. D 48, 4188 (1993); L. Chau, H. Cheng and B. Tseng, Phys. Rev. D 54, 2132 (1996).
[14] A. Datta, University of Hawaii preprint; UH-511-824-95, (1995).
[15] Y. Kubota et al, Nucl. Inst. and Meth. A 320, 66 (1992).
[16] E. Blucher et al, Nucl. Inst. and Meth. A 249, 201 (1989).
[17] P. Avery et al, Phys. Rev. Lett. 71, 2391 (1993).
[18] R. Brun et al. GEANT3, DD/EE/84-1, CERN (1987).
[19] C. Peterson et al., Phys. Rev. D 27, 105 (1993).
[20] P. Avery et al, Phys. Rev. Lett. **75**, 4364-4368 (1995).
[21] K. Edwards et al, Phys. Lett. B 373, 362 (1996).
[22] The Ξ_c^+ selection is identical to that done in Ref [20].
[23] The mass splitting value quoted here should not be construed to mean that the Ξ_c^0 mass is equal to the mass splitting plus the Ξ_c^+ mass quoted in Ref [21].
[24] J. Alexander et al., Phys. Rev. Lett. 74, 3113 (1995) and erratum Phys. Rev. Lett. 74, 4155 (1995).
[25] B. Barish et al, CLNS 97/1470 (1997) (Submitted to Phys. Rev. Lett).
[26] J. Körner, M. Krämer, and D. Pirjol, Prog. Part. Nucl. Phys, Vol 33., pp 787-868 (1994).
[27] T. Bergfeld et al., Phys. Lett. B 323, 229 (1994).
[28] M. B. Voloshin, Phys. Lett. B 385, 369 (1996).
[29] G. Bellini, I. I. Bigi, and P. J. Dornan, PRINT 97-005 (MILAN) to appear in Phys. Rep. (1996).
[30] Henderson et al, Phys. Lett. B 283, 161 (1992).
[31] The analysis in reference [5] measured the reciprocal of B($\Xi_c^0 \to \Xi^- \pi^+ \pi^- \pi^+ / \Xi_c^0 \to \Xi^- \pi^+$).

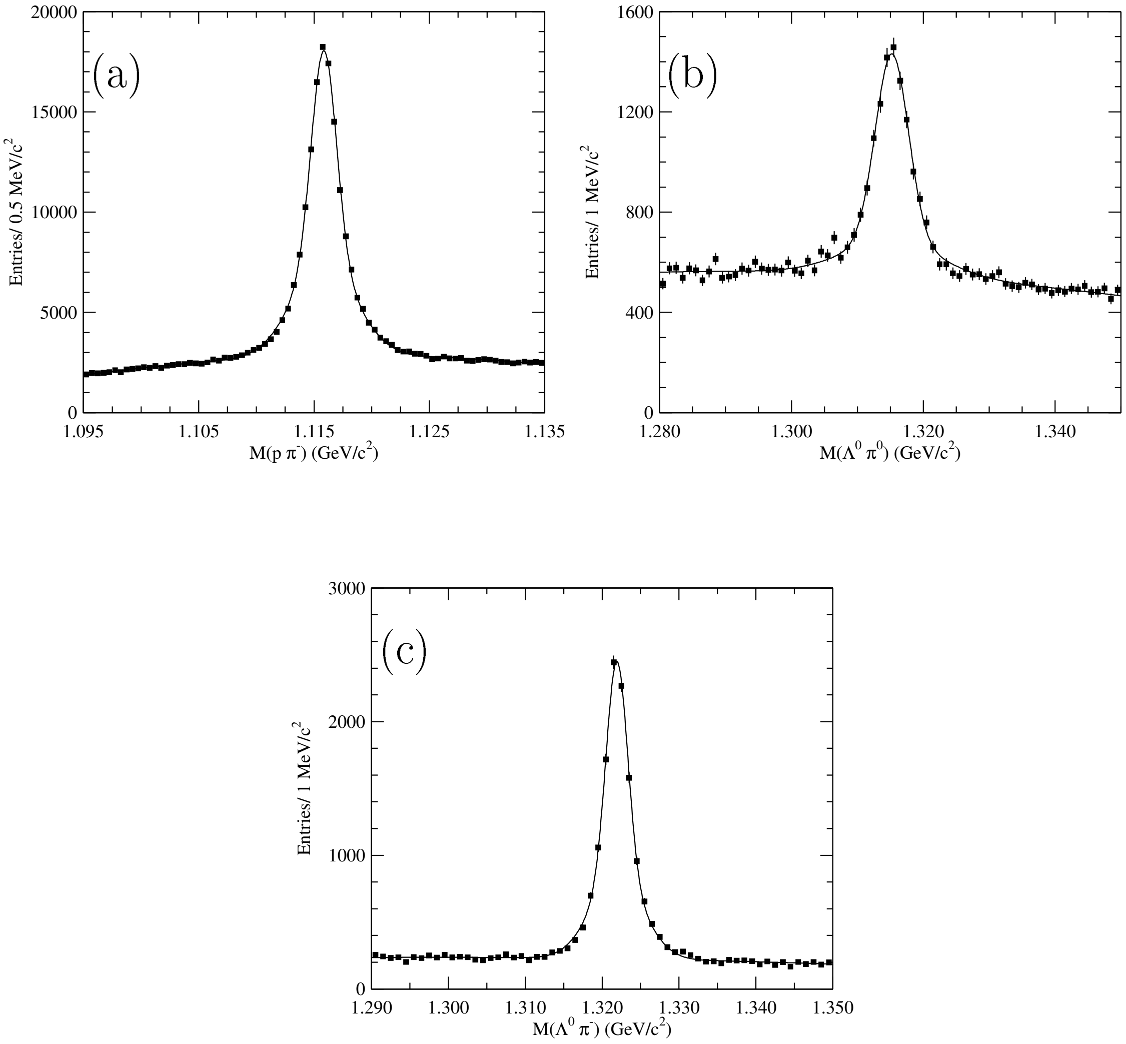

FIG. 1. Invariant mass distribution for (a) $\Lambda\rightarrow p\pi^-$ combinations (b)$\Xi^0\rightarrow\Lambda\pi^0$ combinations (c) $\Xi^-\rightarrow\Lambda\pi^-$ combinations.

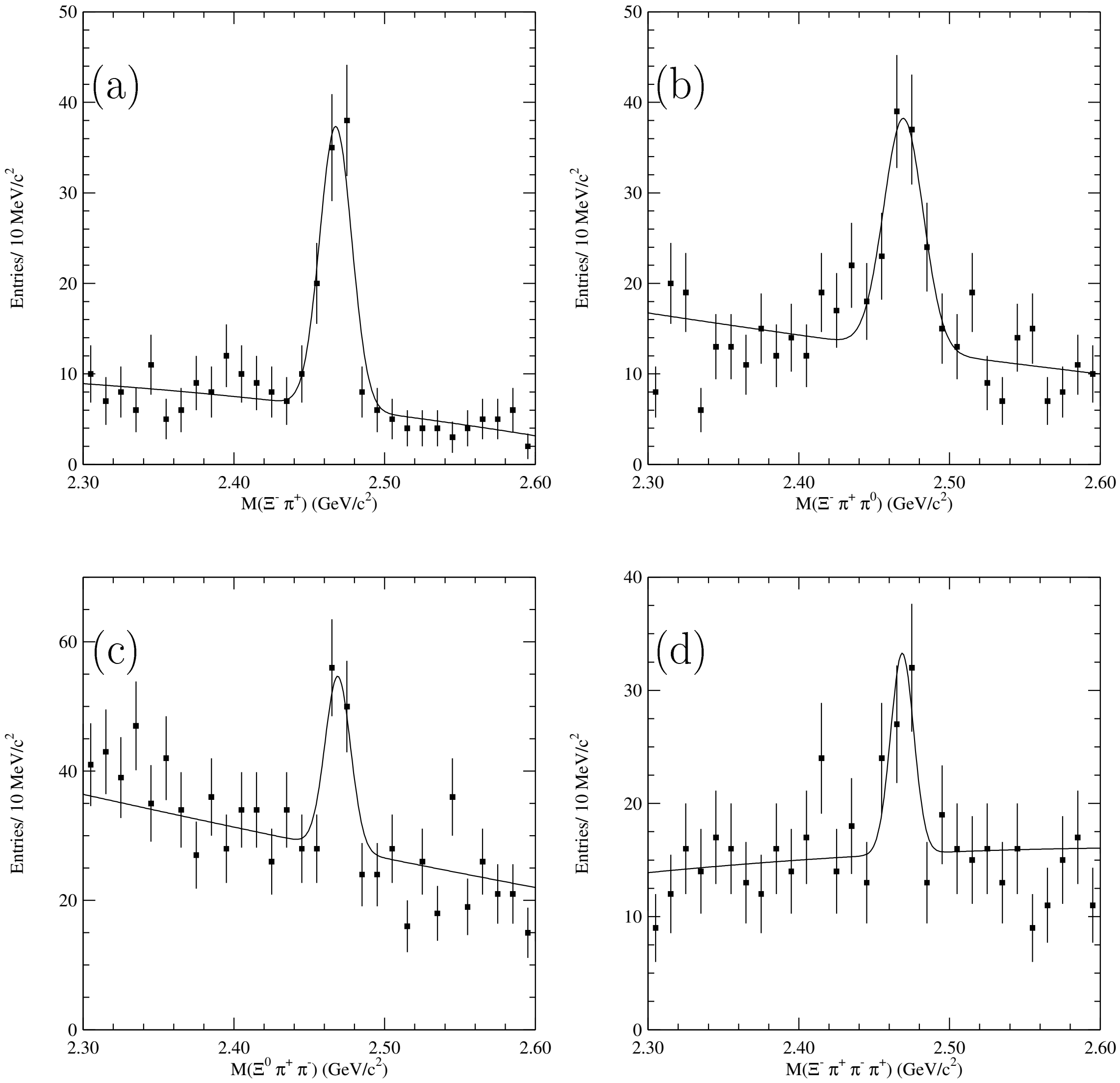

FIG. 2. Invariant mass distributions of Ξ_c^0 decays to the (a) $\Xi^-\pi^+$, (b) $\Xi^0\pi^+\pi^-$, (c) $\Xi^-\pi^+\pi^0$ and (d) $\Xi^-\pi^+\pi^+\pi^-$ modes, with $x_p > 0.5$ for all modes.

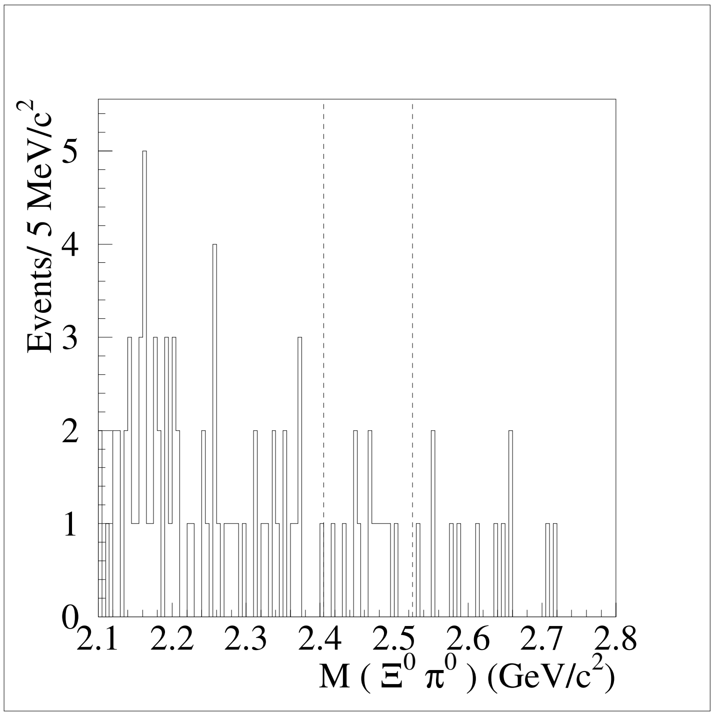

FIG. 3. Invariant mass distribution of $\Xi^0\pi^0$ combinations for $x_p > 0.5$.

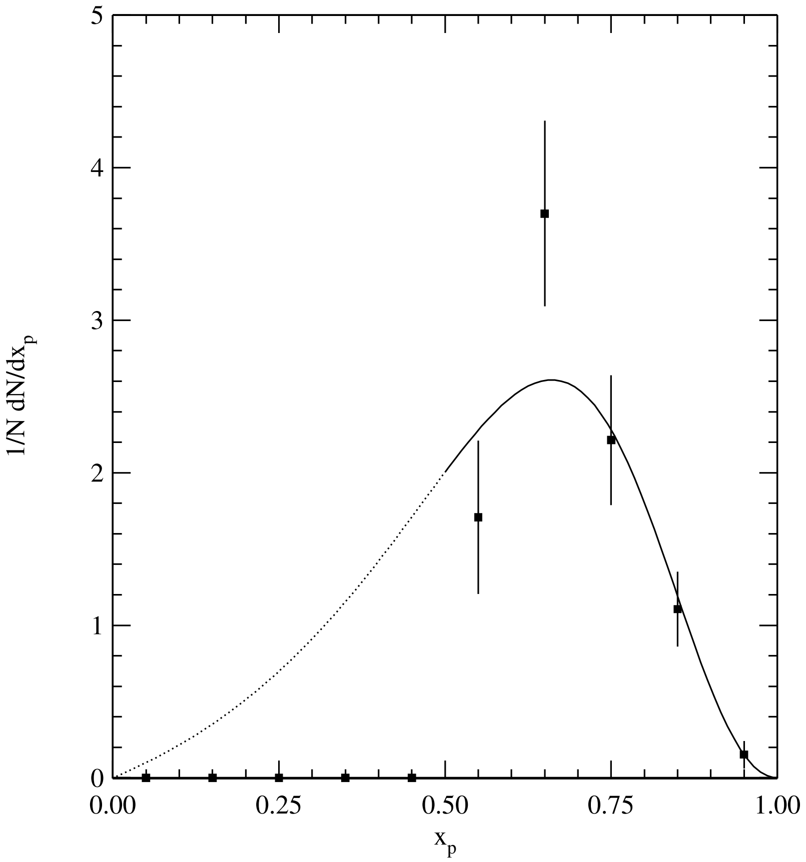

FIG. 4. Normalized momentum distribution $\frac{1}{N}\frac{dN}{dx_p}$ averaged for all four channels, with a fit to the Peterson fragmentation function shown.